moieties of 1 and 2, it seems that interaction of the early metal with the C-O π cloud results in greater bond order reduction than does donation from a lone pair of electrons on oxygen to a Lewis acidic center. Of course, another factor in the comparison of 1 and 2 is the Lewis acidity of the early-metal center. Comparison of the complexes $Cp_2Zr(Me))(\mu\text{-}\eta^1,\eta^1\text{-}OC)Mo(CO)_2Cp$(C-O 1.236 (5) Å, 1545 cm^{-1})[17] and $Cp^*_2Ti(Me)(\mu\text{-}\eta^1,\eta^1\text{-}OC)Mo(CO)_2Cp$(C-O 1.212 (5) Å, 1623 cm^{-1})[15] suggests that Zr(IV) is a more effective Lewis acid than Ti(IV). Thus, it appears both the nature of the CO-metal interaction and the Lewis acidity of the early metal favor C-O bond activation in 1 relative to that in 2.

Acknowledgment. Financial support from the NSERC of Canada is gratefully acknowledged. D.G.D. is grateful for the award of an NSERC of Canada postgraduate scholarship.

Supplementary Material Available: Tables of thermal and hydrogen atom positional parameters and bond distances and angles associated with the cyclopentadienyl rings (6 pages); a listing of values of $10F_o$ and $10F_c$ (18 pages). Ordering information is given on any current masthead page.

(17) De Boer, E. J. M.; De With, J. *J. Organomet. Chem.* **1987**, *320*, 289.

Organometallic Oxides: Preparation, Structure, and Chemical and Physical Properties of Paramagnetic $[(\eta\text{-}C_5H_5)NbCl(\mu\text{-}A)]_3(\mu_3\text{-}OH)(\mu_3\text{-}O)$ (A = Cl, OH) and Other Oxo-Hydroxo Clusters of Niobium†

Frank Bottomley,* Petra N. Keizer, and Peter S. White

Department of Chemistry, University of New Brunswick, Fredericton, New Brunswick, Canada E3B 5A3

Keith F. Preston

Division of Chemistry, National Research Council of Canada, Ottawa, Ontario, Canada K1A 0R9

Received January 17, 1990

Hydrolysis of $Cp'NbCl_4$ ($Cp' = \eta^5\text{-}C_5H_5$ (Cp), $\eta\text{-}C_5H_4Me$ (Cp^1)) in tetrahydrofuran (THF) gave a mixture of products of general formula $[Cp'NbL_4]_2(\mu\text{-}O)$, where L_4 is a combination of H_2O and terminal or bridging Cl that gives eight-coordinate, pentavalent, niobium. For Cp' = Cp, a major constituent of the mixture is $[CpNb(H_2O)Cl_3]_2(\mu\text{-}O)\cdot 2THF\cdot 0.5Et_2O$ (1), the structure of which was determined by X-ray diffraction. Crystal data: monoclinic; $C2/c$; a = 22.105 (4) Å, b = 11.366 (1) Å, c = 15.563 (2) Å, β = 124.71 (1)°; R = 0.056 for 165 parameters and 1444 observed $|F_o|$. The Nb-O-Nb angle in 1 is 173.7 (7)°, and the torsion angle between the $[CpNb(H_2O)Cl_3]$ units is 78.8 (3)°. The H_2O ligands are hydrogen-bonded to lattice THF. Reduction of $[Cp'NbL_4]_2(\mu\text{-}O)$ with aluminum powder gave the cluster $[Cp'NbCl(\mu\text{-}Cl)]_3(\mu_3\text{-}OH)(\mu_3\text{-}O)$ (2). The structure of 2 (Cp' = Cp) as the THF adduct was determined by X-ray diffraction. Crystal data: monoclinic; $P2_1/c$; a = 9.966 (1) Å, b = 12.471 (2) Å, c = 20.321 (2) Å, β = 93.86 (1)°; R = 0.027 for 307 parameters and 3507 observed $|F_o|$. 2 has an isosceles triangle of CpNbCl groups (Nb-Nb = 2.823 (1), 3.239 (1), 3.252 (1) Å) with edge-bridging Cl and face-bridging OH and O ligands. The OH is hydrogen-bonded to the lattice THF. The Nb-Nb distances indicate a single Nb-Nb bond between Nb(1) and Nb(2) but no interaction between Nb(1) or Nb(2) and Nb(3). This model is borne out by the magnetic moment of 2, 1.39 μ_B (295 K), and by the ESR spectrum. The g and ^{93}Nb hyperfine interaction tensors, derived from a spectral analysis of 2, are parallel and axial within experimental error ($g_\parallel$ = 1.9232, $g_\perp$ = 1.9832; $a_\parallel^{93}$ = 649 MHz, $a_\perp^{93}$ = 303 MHz) and show that the unpaired electron is located on Nb(3) in a d_{xy} orbital that makes an angle of approximately 45° to the Nb_3 plane. There is no coupling to the other Nb nuclei or to Cl. Extended Hückel calculations confirm this assignment. The ESR spectrum also shows that 2 exists as two isomers with the proton attached to an oxygen atom either above or below the plane of the Nb atoms. $[Cp'NbCl(\mu\text{-}Cl)]_3(\mu_3\text{-}OH)(\mu_3\text{-}O)$ decomposed slowly in THF solution to give a species formulated as $Cp'_4Nb_5Cl_5(OH)_9O(THF)_2$ (5) on the basis of spectroscopy, analysis, and a partial structure determination; 5 has an adamantane-like $Nb_4(OH)_6$ core and a magnetic moment of 1.86 μ_B. Reduction of $[CpNbL_4]_2(\mu\text{-}O)$ with zinc powder gave units of $[CpNbCl(\mu\text{-}OH)]_3(\mu_3\text{-}OH)(\mu_3\text{-}O)$ (3) connected by ZnCl(OH)(THF). Spectroscopic and magnetic methods establish that 3 has a structure similar to that of 2, with edge-bridging OH instead of Cl.

Introduction

We are synthesizing cyclopentadienylmetal oxides that retain the properties of conventional metal oxides but are soluble in nonpolar solvents. Three general routes to such oxides may be envisaged. The first is oxidation of a cyclopentadienylmetal complex by a source of oxygen. The second is treatment of a metal oxide with a cyclopentadienyl salt. The third is to aggregate a mononuclear or low polynuclear cyclopentadienylmetal oxo complex. We have had considerable success with the first method, obtaining clusters such as $Cp_{14}V_{16}O_{24}$,[1] $[CpV]_5(\mu_3\text{-}O)_6$,[2,3] and

† Issued as NRC No. 31257.

(1) Bottomley, F.; Paez, D. E.; White, P. S. *J. Am. Chem. Soc.* **1985**, *107*, 7226.

0276-7333/90/2309-1916$02.50/0

$[CpCr(\mu_3\text{-}O)]_4$[3,4] (Cp = η-C_5H_5) by oxidation of Cp_2V or Cp_2Cr. This method cannot be used for the second- and third-row congeners of these elements because the appropriate Cp_2M species have, at best, only a transitory existence. We have had little success with the second method as yet, probably because of the thermodynamic stability of metal oxides. We therefore turned to the third method, for which a suitable strategy of aggregation is required. Since most mono- or dinuclear cyclopentadienylmetal oxo complexes have the metal in a high oxidation state (IV–VII), whereas in the above vanadium and chromium oxides the formal oxidation states are III/IV, reductive aggregation was an attractive possibility. Such reductive aggregation was employed by Floriani and co-workers in the synthesis of $[CpTi]_6(\mu_3\text{-}Cl)_n(\mu_3\text{-}O)_{8-n}$ (n = 0, 2, 4) by reduction of $[CpTiCl(\mu\text{-}O)]_4$ or $[CpTiCl_2]_2(\mu\text{-}O)$.[5]

Because of our previous success in preparing cyclopentadienylmetal oxides of vanadium and chromium, our efforts have been directed to these metals and to their congeners niobium and molybdenum. We report here the synthesis and physical and chemical properties of the trinuclear, paramagnetic cyclopentadienylniobium chloride oxides $[Cp'NbCl(\mu\text{-}A)]_3(\mu_3\text{-}OH)(\mu_3\text{-}O)$ (A = Cl, OH; Cp' = Cp, η-C_5H_4Me (Cp^1)). During the writing of the present paper Curtis and Real described the structure of $[Cp^1NbCl(\mu\text{-}Cl)]_3(\mu_3\text{-}Cl)(\mu_3\text{-}O)$, obtained in low yield on decarbonylation of $[Cp^1Nb(CO)_2(\mu\text{-}Cl)]_2$.[6]

Results and Discussion

An excellent entry into cyclopentadienylniobium oxides appeared to be $Cp'NbCl_2(O)$, (Cp' = Cp, MeCp, Cp* (= η^5-$C_5(CH_3)_5$)), the Nb analogue of the earliest known cyclopentadienylmetal oxide, $Cp'VCl_2(O)$.[7-13] Several syntheses of $Cp'VCl_2(O)$ are available, but all start from either Cp'_2V, the niobium analogue of which is not available, or $Cp'V(CO)_4$, the niobium analogue of which is only available in reasonable yield when extremely high pressures and temperatures are used.[14] An alternative route appeared to be treatment of the readily available $Cp'NbCl_4$[15] with Ag_2O or Ag_2CO_3, reagents that we have used previously to convert chloro derivatives of Cp'V into oxo complexes.[11] However, there was no reaction between $CpNbCl_4$ and Ag_2O or Ag_2CO_3, even under forcing conditions. We therefore turned to hydrolysis. Other workers have also explored the hydrolysis of $Cp'MCl_4$ (M = Nb,[16-19] Ta[20]).

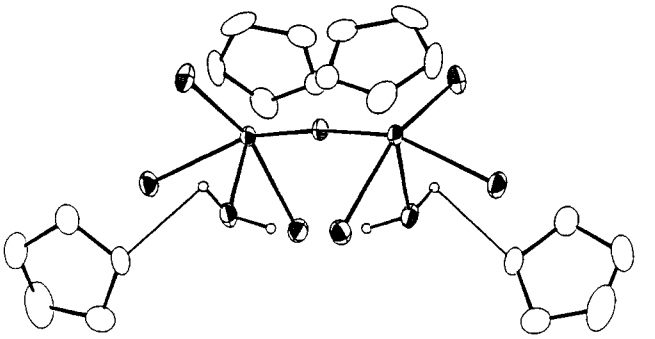

Figure 1. Molecular structure of $[CpNb(H_2O)Cl_3]_2(\mu\text{-}O)\cdot 2THF$ (1) as determined by X-ray diffraction.

Table I. Important Distances (Å) and Angles (deg) in $[CpNb(H_2O)Cl_3]_2(\mu\text{-}O)\cdot 2THF\cdot 0.5Et_2O$

Nb–O(1)	1.915 (1)	Nb–Cp[a]	2.133 (15)
Nb–O(2)	2.189 (9)	O(2)–O(3)	2.612 (12)
Nb–Cl(1)	2.443 (3)	O(3)–H(2)	2.29
Nb–Cl(2)	2.436 (4)	Cl(3)–H(2A)	2.13
Nb–Cl(3)	2.486 (4)		
Nb–O(1)–Nb	173.7 (1)	O(2)–Nb–Cl(3)	76.8 (3)
O(1)–Nb–O(2)	77.6 (3)	O(2)–Nb–Cp	177.3 (5)
O(1)–Nb–Cl(1)	153.8 (3)	Cl(1)–Nb–Cl(2)	87.1 (1)
O(1)–Nb–Cl(2)	89.0 (2)	Cl(1)–Nb–Cl(3)	85.6 (1)
O(1)–Nb–Cl(3)	87.4 (3)	Cl(1)–Nb–Cp	102.7 (4)
O(1)–Nb–Cp	103.4 (4)	Cl(2)–Nb–Cl(3)	155.7 (1)
O(2)–Nb–Cl(1)	76.2 (2)	Cl(2)–Nb–Cp	103.5 (4)
O(2)–Nb–Cl(2)	78.9 (3)	Cl(3)–Nb–Cp	100.7 (4)

[a] Cp is the centroid of the η-C_5H_5 ring.

Hydrolysis of $Cp'NbCl_4$. When $Cp'NbCl_4$ was hydrolyzed in tetrahydrofuran solution (1:1 molar ratio of H_2O:Nb), a yellow-brown product was obtained, either by precipitating with ether after 2 h or on setting the tetrahydrofuran solution aside for several days. Analytical evidence consistently suggested the empirical formula $Cp'_2Nb_2Cl_4O_2(H_2O)_3\cdot THF$ (i.e. $Cp'NbCl_2(O)\cdot 2S$, where S = solvent) for this material. However, the physical and chemical properties clearly indicated that it was a mixture of compounds. An important component of the mixture was yellow $[Cp'Nb(H_2O)Cl_3]_2(\mu\text{-}O)$ (1), which was isolated as the bis THF adduct for Cp' = Cp and characterized fully by X-ray diffraction (Figure 1). In addition to the two THF molecules shown in Figure 1, there is half of a molecule of ether for each molecule of 1 in the lattice.

Royo and co-workers identified $[CpNbCl_2(\mu\text{-}Cl)]_2(\mu\text{-}O)$ as being the product that was formed initially from $CpNbCl_4$ and "wet dichloromethane" and 1 as being the ultimate product under such conditions.[18] Green, Prout, and co-workers obtained the Cp^1 derivative of 1 by hydrolysis of Cp^1NbCl_4 under unspecified conditions.[16,17] Our results indicate that hydrolysis of $Cp'NbCl_4$ gives a mixture of compounds of general formula $[Cp'NbL_4]_2(\mu\text{-}O)$, where L_4 is a combination of H_2O and terminal or bridging Cl such that the niobium remains eight-coordinate and pentavalent. An important constituent of the mixture is $[Cp'Nb(H_2O)Cl_3]_2(\mu\text{-}O)$.

The structure of 1 (see Figure 1 and Table I) is very similar to that of $[Cp^1Nb(H_2O)Cl_3]_2(\mu\text{-}O)$ as determined

(2) Bottomley, F.; White, P. S. *J. Chem. Soc., Chem. Commun.* **1981**, 28.
(3) Bottomley, F.; Paez, D. E.; White, P. S. *J. Am. Chem. Soc.* **1982**, *104*, 5651.
(4) Bottomley, F.; Paez, D. E.; White, P. S. *J. Am. Chem. Soc.* **1981**, *103*, 5581.
(5) Roth, A.; Floriani, C.; Chiesi-Villa, A.; Guastini, C. *J. Am. Chem. Soc.* **1986**, *108*, 6823.
(6) Curtis, M. D.; Real, J. *Inorg. Chem.* **1988**, *27*, 3176.
(7) Fischer, E. O.; Vigoureux, S. *Chem. Ber.* **1958**, *91*, 1342.
(8) Fischer, E. O.; Vigoureux, S.; Kuzel, P. *Chem. Ber.* **1960**, *93*, 701.
(9) De Liefde Meijer, H. J.; Van der Kerk, G. J. M. *Recl. Trav. Chim. Pays-Bas* **1965**, *84*, 1418.
(10) Bottomley, F.; Darkwa, J.; Sutin, L. C.; White, P. S. *Organometallics* **1986**, *5*, 2165.
(11) Bottomley, F.; Sutin, L. *J. Chem. Soc., Chem. Commun.* **1987**, 1112.
(12) Herrmann, W. A.; Weichselbaumer, G.; Kneuper, H.-J. *J. Organomet. Chem.* **1987**, *319*, C21.
(13) Herberhold, M.; Kremnitz, W.; Kuhnlein, M.; Ziegler, M. L.; Brunn, K. *Z. Naturforsch.* **1987**, *42B*, 1520.
(14) Herrmann, W. A.; Biersack, H. *J. Organomet. Chem.* **1980**, *19*, 397.
(15) Bunker, M. J.; De Cian, A.; Green, M. L. H.; Moreau, J. J. E.; Siganporia, N. *J. Chem. Soc., Dalton Trans.* **1980**, 2155.
(16) Daran, J.-C.; Prout, K.; De Cian, A.; Green, M. L. H.; Siganporia, N. J. *J. Organomet. Chem.* **1977**, *136*, C4.
(17) Prout, K.; Daran, J.-C. *Acta Crystallogr.* **1979**, *B35*, 2882.
(18) Andreu, A. M.; Jalon, F. A.; Otero, A.; Royo, P.; Manotti-Lanfredi, A. M.; Tiripicchio, A. *J. Chem. Soc., Dalton Trans.* **1987**, 953. Jalon, F. A.; Otero, A.; Royo, P.; Fernandez-G., J. M.; Rosales, M. J.; Toscano, R. A. *J. Organomet. Chem.* **1987**, *331*, C4.
(19) Andreu, A. M.; Jalon, F. A.; Otero, A. *J. Organomet. Chem.* **1988**, *353*, 185.
(20) Jernakoff, P.; de Meric de Bellefon, C.; Geoffroy, G. L.; Rheingold, A. L.; Geib, S. J. *Organometallics* **1987**, *6*, 1362.

Table II. Important Distances (Å) and Angles (deg) in $[CpNbCl(\mu\text{-}Cl)]_3(\mu_3\text{-}OH)(\mu_3\text{-}O)\cdot THF$ (Esd's in Parentheses)

Nb(1)–Nb(2)	2.823 (1)	Nb(2)–Cl(2)	2.565 (1)
Nb(1)–Nb(3)	3.239 (1)	Nb(2)–Cl(3)	2.536 (1)
Nb(2)–Nb(3)	3.252 (1)	Nb(2)–Cl(5)	2.456 (1)
Nb(1)–O(1)	2.201 (3)	Nb(2)–C(B)[a]	2.107 (3)
Nb(1)–O(2)	2.079 (3)	Nb(3)–O(1)	2.231 (3)
Nb(1)–Cl(1)	2.549 (1)	Nb(3)–O(2)	2.060 (3)
Nb(1)–Cl(3)	2.518 (1)	Nb(3)–Cl(1)	2.503 (1)
Nb(1)–Cl(4)	2.444 (1)	Nb(3)–Cl(2)	2.519 (1)
Nb(1)–C(A)[a]	2.107 (3)	Nb(3)–Cl(6)	2.426 (1)
Nb(2)–O(1)	2.171 (3)	Nb(3)–C(C)[a]	2.102 (3)
Nb(2)–O(2)	2.082 (3)	O(1)–H(1)	0.94 (6)
Cl(1)–Nb(1)–Cl(3)	151.19 (4)	Cl(2)–Nb(2)–C(B)[a]	102.2
Cl(2)–Nb(2)–Nb(3)	152.67 (4)	Cl(3)–Nb(2)–C(B)	104.5
Cl(1)–Nb(3)–Cl(2)	151.43 (4)	Cl(5)–Nb(2)–C(B)	105.7
Nb(1)–Cl(1)–Nb(3)	79.72 (4)	O(1)–Nb(2)–C(B)	171.8
Nb(2)–Cl(2)–Nb(3)	79.54 (3)	O(2)–Nb(2)–C(B)	108.5
Nb(1)–Cl(3)–Nb(2)	67.92 (3)	Cl(1)–Nb(1)–C(C)[a]	101.9
Cl(2)–Nb(3)–C(A)[a]	102.7	Cl(3)–Nb(1)–C(C)	105.8
Cl(1)–Nb(3)–C(A)	103.9	Cl(4)–Nb(1)–C(C)	106.4
Cl(6)–Nb(3)–C(A)	104.9	O(1)–Nb(1)–C(C)	170.2
O(1)–Nb(3)–C(A)	105.6	O(2)–Nb(1)–C(C)	107.4
O(2)–Nb(3)–C(A)	169.9		

[a] C(A), C(B), and C(C) are the centroids of rings A, B, and C, respectively.

by Prout and Daran.[17] In **1**, each of the water ligands is hydrogen-bonded to lattice THF molecules, whereas $[Cp^1Nb(H_2O)Cl_3]_2(\mu\text{-}O)$ has intermolecular hydrogen bonding of H_2O to Cl, forming a chain structure. The torsion angle between the Nb–H_2O vectors (which are approximately trans to Cp) is 78.8 (3)° in **1** and is essentially the same (75.1°) in $[Cp^1Nb(H_2O)Cl_3]_2(\mu\text{-}O)$, despite the different types of hydrogen bonding. This torsion angle, coupled with the short Nb–O distance to the bridging oxygen (1.915 (1) Å) and the almost linear Nb–O–Nb unit (173.7 (7)°), indicates significant π-bonding between the bridging oxygen and the niobium atoms.[21,22]

Reduction of $[Cp'NbL_4]_2(\mu\text{-}O)$. Reduction of $[Cp'NbL_4]_2(\mu\text{-}O)$ with aluminum powder in THF was slow and gave a mixture of $[Cp'NbCl(\mu\text{-}Cl)]_3(\mu_3\text{-}OH)(\mu_3\text{-}O)$ (**2**) and unreduced **1**. The structure of **2**, as the THF adduct, was determined by X-ray diffraction for Cp′ = Cp (Figure 2 and Table II). It appeared that reduction of **1** was slower than reduction of the other constituent(s) of the $[Cp'NbL_4]_2(\mu\text{-}O)$ mixture, since only **1** and **2** were present after 48 h. Reduction with Al/$AlCl_3$ proceeded, surprisingly, slower than with aluminum alone. However, $AlCl_3$ appeared to catalyze the decomposition of **2**, as discussed below. For some obscure reason, reduction of $[CpNbL_4]_2(\mu\text{-}O)$ with aluminum gave **2** as the THF adduct (Figure 2), whereas reduction with Al/$AlCl_3$ gave an unsolvated form of **2** with a structure similar to that of the Cp^1 derivative determined by Curtis and Real.[6]

Reduction of $[CpNbL_4]_2(\mu\text{-}O)$ with zinc powder was rapid, and the reduction went to completion. The product was characterized as containing $[CpNbCl(\mu\text{-}OH)]_3(\mu_3\text{-}OH)(\mu_3\text{-}O)$ (**3**), but the characterization was complicated by the retention of Zn^{2+}, making this reduction unsuitable as a general method of preparation.

Reduction of $[CpNbL_4]_2(\mu\text{-}O)$ with sodium amalgam gave $[CpNbCl(\mu\text{-}OH)]_3(\mu_3\text{-}OH)(\mu_3\text{-}O)$ (**3**), as with zinc reduction. However, the reaction with Na/Hg was significantly slower than with zinc, and workup of the product was complicated by the presence of mercury. Sodium metal alone did not reduce $[CpNbL_4]_2(\mu\text{-}O)$.

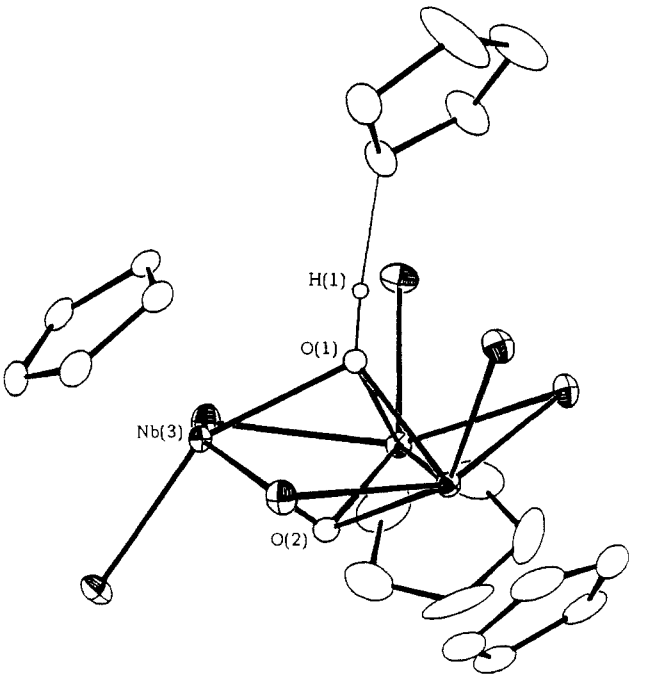

Figure 2. Molecular structure of $[CpNbCl(\mu\text{-}Cl)]_3(\mu_3\text{-}OH)(\mu_3\text{-}O)\cdot THF$ (**2**) as determined by X-ray diffraction.

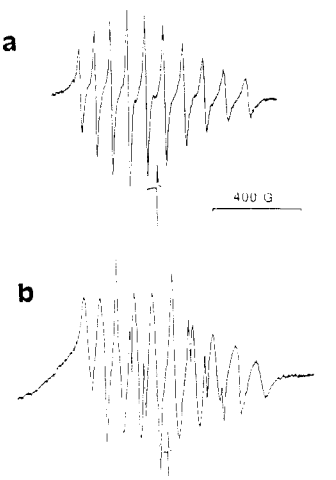

Figure 3. Electron spin resonance spectra of $[CpNbCl(\mu\text{-}A)]_3(\mu_3\text{-}OH)(\mu_3\text{-}O)$ at 295 K (THF solution): (a) A = Cl; (b) A = OH. The sharp lines in (b) are due to a minor contribution of **5** to the spectrum of **3**.

The trinuclear clusters **2** and **3** could not be reduced further with $LiAlH_4$ or $NaBH_4$, but sodium amalgam or sodium naphthalenide reduced red-brown **3** to a chocolate brown species. This was insoluble in nonpolar organic solvents and only dissolved, with reaction, in methanol.

Decomposition of $[Cp'NbCl(\mu\text{-}Cl)]_3(\mu_3\text{-}OH)(\mu_3\text{-}O)$. The cluster **2** decomposed slowly in THF solution. The decomposition was most thoroughly investigated for $[Cp^1NbCl(\mu\text{-}Cl)]_3(\mu_3\text{-}OH)(\mu_3\text{-}O)$ and could be conveniently followed by using the ESR spectrum at 298 K. In essence, the characteristic 10-line spectrum of **2** (Figure 3a) disappeared over a period of 5–8 days at 25 °C, being replaced by a very broad envelope, accompanied by a 10-line spectrum that was not due to **2**. The changes in the ESR spectrum indicated either that **2** converted to compound **4** (which shows a broad ESR signal), and **4** decomposed to **5** (which shows a 10-line ESR signal and is probably $Cp'_4Nb_5Cl_5(OH)_9O(THF)_2$ (see below)), or that **2** decom-

(21) Prout, K.; Cameron, T. S.; Forder, R. A.; Critchley, R.; Denton, B.; Rees, G. V. *Acta Crystallogr.* **1974**, *B30*, 2290.
(22) Skirpkin, Yu. V.; Eremenko, I. L.; Pasynskii, A. V.; Volkov, O. G.; Bakum, S. I.; Porai-Koshits, M. A.; Antsyshkina, A. S.; Dikareva, L. M.; Ostrikova, V. N.; Sahkarov, S. G.; Struchkov, Yu. T. *Sov. J. Coord. Chem. (Engl. Transl.)* **1985**, *11*, 570.

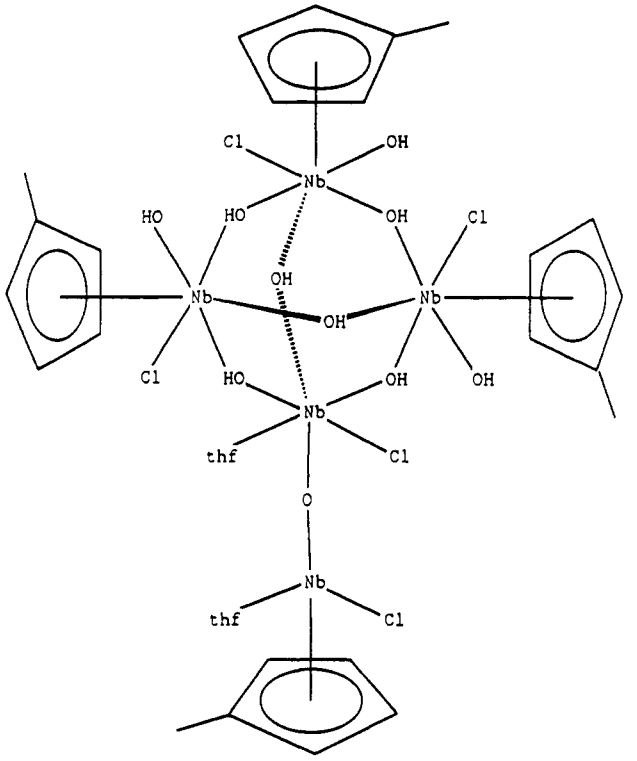

Figure 4. Proposed structure of $Cp^1_4Nb_5Cl_5(OH)_9O(THF)_2$ (5).

posed directly to 4 and 5. The decomposition of 2 was catalyzed by Al^{3+}, as was apparent when $AlCl_3$ was added during the reduction of $[Cp'NbL_4]_2(\mu\text{-}O)$.

A green-brown material was isolated from the decomposition in THF. Analytical, spectroscopic, magnetic, and molecular weight evidence, combined with a partial structure determination by X-ray diffraction, suggested that this compound had the formula $Cp^1_4Nb_5Cl_5(OH)_9O(THF)_2$. A reasonable structure is shown in Figure 4. The adamantane-like $Nb_4(O)_6$ unit, with an Nb attached to it by O, was clearly identified. Because of the very poor intensity data (see Experimental Section), and also problems of disorder between the Cl and OH and between THF and Cp^1, it was not possible to uniquely define the terminal ligands or to distinguish between O and OH. The assignment of the ligands shown in Figure 4 was made to conform to the other evidence and to considerations of valency and magnetism.

The magnetic moment of $Cp^1_4Nb_5Cl_5(OH)_9O(THF)_2$ was 1.86 μ_B at 293 K (Evans method,[23] THF solution), indicating only one unpaired electron in the pentanuclear cluster. Therefore, this compound is probably 5, the one with the 10-line ESR signal. Compound 4 is then assigned the broad featureless ESR signal. However, 4 was never isolated in a pure state and its structure is unknown.

Structure of $[CpNbCl(\mu\text{-}Cl)]_3(\mu_3\text{-}OH)(\mu_3\text{-}O)\cdot THF$ (2) As Determined by X-ray Diffraction. The trinuclear cluster 2 has a structure very similar to that of the Cp^1 analogue described by Curtis and Real,[6] with the exception of the hydrogen bonding, which is important to its properties. It consists of an isosceles triangle of Nb atoms (Nb(1)–Nb(2) = 2.823 (1) Å, Nb(3)–Nb(1) = 3.239 (1) Å, Nb(3)–Nb(2) = 3.252 (1) Å) with edge-bridging Cl ligands; each Nb atom carries a Cp and a terminal Cl ligand, and the Nb_3 triangle has an O atom capping one face and an OH capping the other (see Figure 2 and Table II). The Cl atoms bridging the nonbonded Nb(1)–Nb(3) and Nb(2)–Nb(3) edges are essentially in the plane of the triangle, whereas Cl(3), which bridges the Nb(1)–Nb(2) edge, is 1.19 Å out of the plane. The displacement is away from the Cp rings and toward the terminal Cl ligands, presumably for steric reasons. There is an approximate plane of symmetry passing through Nb(3), Cl(3), Cl(6), and the μ_3-OH and O ligands (Table III).

Table III. Important Planes, and Distances (Å) of Atoms from Them, in $[CpNbCl(\mu\text{-}Cl)]_3(\mu_3\text{-}OH)(\mu_3\text{-}O)\cdot THF$

Plane 1: [2.1652 (19)]x + [10.5292 (11)]y + [9.634 (3)]z = 5.1747 (4)			
Nb(1–3)	0.000	Cl(1)	0.149 (1)
O(1)	−1.267 (3)	Cl(2)	0.249 (1)
O(2)	1.024 (3)	Cl(3)	−1.194 (1)
Plane 2: [9.8356 (12)]x − [1.688 (6)]y − [3.136 (12)]z = 1.826 (3)			
Nb(3)	0.001 (1)	Nb(1)	−1.356 (1)
O(1)	−0.009 (3)	Nb(2)	1.463 (1)
O(2)	0.095 (3)	Cl(1)	−2.406 (1)
Cl(3)	−0.008 (2)	Cl(2)	2.457 (1)
Cl(6)	−0.020 (2)	Cl(4)	−2.797 (2)
		Cl(5)	−2.671 (2)
		C(A)[a]	−2.413
		C(B)[a]	2.579

[a] C(A) and C(B) are the centroids of rings A and B, respectively.

The assignment of O(1)H(1) as a μ_3-hydroxide, rather than as an oxide, was confirmed by observation of the hydrogen atom (H(1)) in a difference Fourier synthesis, as well as by inference from the Nb–O distances and angles and from the spectroscopic results. The hydrogen is quite strongly bonded to the oxygen of the lattice THF (O(3)–H(1) = 1.75 Å, O(1)–O(3) = 2.691 (4) Å; O(1)–H(1)–O(3) = 178°). In the solid state the hydrogen bonding causes the isomerism discussed below and significant differences in the ESR spectrum from those described by Curtis and Real.[6]

The gross structure of 2 is similar to those of $[Cp^*ZrCl(\mu\text{-}OH)]_3(\mu_3\text{-}OH)(\mu_3\text{-}O)$[24] and $\{[Cp^*TaCl][Cp^*Ta(H_2O)]_2(\mu_2\text{-}O)_3(\mu_3\text{-}O)_2\}^+$[20,25] as well as the alkoxy derivatives $[Mo(OCH_2CMe_3)_2(\mu\text{-}OCH_2CMe_3)]_3(\mu_3\text{-}OCH_2CMe_3)(\mu_3\text{-}O)$,[26] $[U(OCMe_3)_2(\mu\text{-}OCMe_3)]_3(\mu_3\text{-}OCMe_3)(\mu_3\text{-}O)$,[27] and $[Y(OCMe_3)_2][Y(OCMe_3)(THF)]_2(\mu\text{-}OCMe_3)_3(\mu_3\text{-}OCMe_3)(\mu_3\text{-}Cl)$.[28] An important difference is that these have equilateral triangles of metal atoms with the edge-bridging groups all in the plane of the triangle.[29] The distances for Zr–Zr (average 3.229 Å[24]), Ta–Ta (average 3.092 Å[20]), U–U (average 3.574 (1) Å[27]), and Y–Y (average 3.584 Å[28]) are indicative of nonbonding interactions, as would be expected for d^0 metals. The Mo–Mo distances (average 2.529 (9) Å[26]), on the other hand, are appropriate for a single bond, and six electrons are available in diamagnetic $[Mo(OCH_2CMe_3)_2(\mu\text{-}OCH_2CMe_3)]_3(\mu_3\text{-}OCH_2CMe_3)(\mu_3\text{-}O)$ to form these bonds. In 2 there is a single bond between Nb(1) and Nb(2) (2.823 (1) Å) and no bonds between Nb(3) and Nb(1) or Nb(2) (3.239 (1) and 3.252 (1) Å).

(23) Evans, D. F.; Fazakerley, G. V.; Phillips, R. F. *J. Chem. Soc. A* **1971**, 1931.

(24) Babcock, L. M.; Day, V. W.; Klemperer, W. G. *J. Chem. Soc., Chem. Commun.* **1988**, 519; *Inorg. Chem.* **1989**, *28*, 806.

(25) The evidence presented in ref 20 does not uniquely define the formula $\{[Cp^*TaCl][Cp^*Ta(H_2O)]_2(\mu_2\text{-}O)_3(\mu_3\text{-}O)_2\}^+$. A formula such as $\{[Cp^*TaCl][Cp^*Ta(H_2O)][Cp^*Ta(OH)](\mu_2\text{-}OH)(\mu_2\text{-}O)_2(\mu_3\text{-}O)_2\}^+$, among others, would fit the data.

(26) Chisholm, M. H.; Folting, K.; Huffman, J. C.; Kirkpatrick, C. C. *J. Am. Chem. Soc.* **1981**, *103*, 5967.

(27) Cotton, F. A.; Marler, D. O.; Schwotzer, W. *Inorg. Chim. Acta* **1984**, *95*, 207.

(28) Evans, W. J.; Sollberger, M. S.; Hanusa, T. P. *J. Am. Chem. Soc.* **1988**, *110*, 1841.

(29) In $[Y^a(OCMe_3)_2][Y^b(OCMe_3)(THF)]_2(\mu\text{-}OCMe_3)_3(\mu_3\text{-}OCMe_3)(\mu_3\text{-}Cl)$[28] there is a slight distortion of the equilateral triangle, the two Y^a–Y^b distances being 3.628 Å and the Y^b–Y^b distance being 3.497 Å. This difference is probably caused by the different terminal ligands attached to Y^a and Y^b.

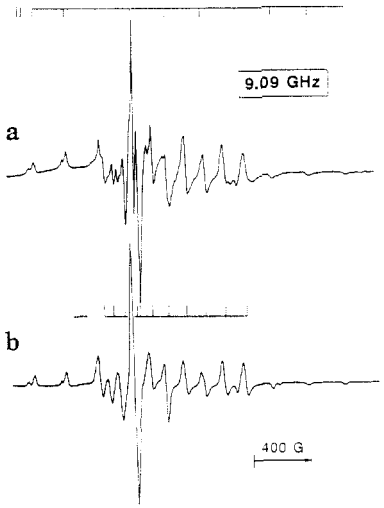

Figure 5. Electron spin resonance spectrum of [CpNbCl(μ-Cl)]$_3$(μ_3-OH)(μ_3-O) at 110 K (a) and the simulated spectrum (b) (frozen THF solution).

As discussed below, there is clear evidence that in solution the proton may be attached to either O(1) or O(2). Attachment to O(2) would require lengthening of all Nb–O(2) distances by ca. 0.13 Å and shortening of the Nb–O(1) distances by the same amount. Considerable disorder in the crystal would occur if a mixture of the two isomers was present; no evidence of such disorder was found. The lattice THF probably determines which isomer is observed in the crystal. Hydrogen bonding between O(2) and THF would be severely hampered by the steric repulsion of the two Cp rings on the same side of the plane of the three Nb atoms as O(2). However, Curtis and Real observed the same isomer as for **2**, though their crystal was not solvated.[6]

Characterization of [CpNbCl(μ-OH)]$_3$(μ_3-OH)(μ_3-O) (3). Despite many attempts with both the Cp and Cp^1 derivatives, crystals of the product of the reduction of [CpNbL$_4$]$_2$(μ-O) with zinc powder were never obtained. The product was characterized as {[CpNbCl(μ-OH)]$_3$(μ_3-OH)(μ_3-O)}$_2$(ZnCl(OH)(THF)) on the basis of elemental analyses, molecular weight determination by osmometry, infrared, NMR, ESR (see Figures 3b and 6a), and mass spectroscopies and by analogy with **2**. Because of the retention of Zn^{2+} it is difficult to distinguish between the isomers [CpNbCl(μ-OH)]$_3$(μ_3-OH)(μ_3-O) and [CpNb(OH)(μ-Cl)]$_3$(μ_3-OH)(μ_3-O) by spectroscopy. However, the ESR spectrum was extremely similar to that of [CpNbCl(μ-Cl)]$_3$(μ_3-OH)(μ_3-O). A detailed account of the latter spectrum and its interpretation is given below. Here we note that the ESR spectra show that **2** and **3** have virtually identical electronic structures, although **3** has somewhat lower g values and a substantially greater line width (75 compared to 30 MHz; compare Figures 5a and 6a). Terminal OH ligands would be expected to be freely rotating, even at 110 K, and to contribute less by way of unresolved ^{1}H superhyperfine interaction to the line width than rigid bridging OH ligands. The greater line width therefore suggests that **3** is [CpNbCl(μ-OH)]$_3$(μ_3-OH)(μ_3-O). The minor component evident (Figure 3b) in the isotropic spectrum of **3** has a sharp 10-line spectrum with parameters (g_{iso} = 1.9760, a_{iso} = 327 MHz) identical within experimental error with those of **5**. From the relative peak heights and line widths, we estimate that this component represents no more than a 3% contaminant. We do not anticipate, therefore, that its presence will significantly affect the spectral analyses of **3**.

The formation of [Cp′NbCl(μ-OH)]$_3$(μ_3-OH)(μ_3-O) from [Cp′NbL$_4$]$_2$(μ-O) requires a source of oxygen, since the

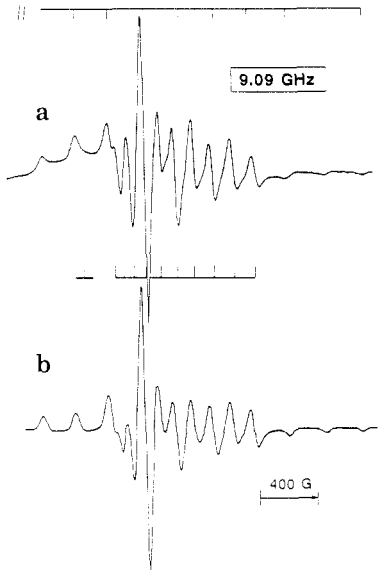

Figure 6. Electron spin resonance spectrum of [CpNbCl(μ-OH)]$_3$(μ_3-OH)(μ_3-O) at 110 K (a) and the simulated spectrum (b) (frozen THF solution).

product has 1.67 O per Nb whereas the starting material has, at maximum, 1.50. A redistribution reaction among the niobium complexes could be occurring, but the strength of the Nb–O bond makes this unlikely. A more probable source of oxygen is the zinc oxide coating that cannot be removed from the surface of the zinc powder used in the reduction.

Magnetic and Electron Spin Resonance Properties of [CpNbCl(μ-A)]$_3$(μ_3-OH)(μ_3-O) (A = Cl, OH). In a formal sense **2** and **3** contain three Nb(IV), d^1, ions. The structural data for **2** show that two of the three electrons of the Nb$_3$ unit are paired in a bond between Nb(1) and Nb(2). This would leave a single unpaired electron. The magnetic moment of **2** (Evans method,[23] THF solution) was 1.39 μ_B and of **3** was 1.33 μ_B, both at 295 K. The values are considerably lower than the spin-only value for a single electron, 1.73 μ_B, but are in line with those generally observed for Nb(IV) compounds, 1.1–1.7 μ_B.[30] The low values are due to spin–orbit coupling. The isotropic ESR spectra of **2** and **3** at 295 K are shown in parts a and b of Figure 3, respectively (the spectrum of **3** shows a minor component assigned to a small amount of **5**, as discussed above). Curtis and Real apparently observed a similar spectrum for **2**, although no details were given.[6] The observation of well-resolved 10-line spectra at room temperature in THF solution again indicates an $S = {}^1/_2$ system and suggests that the single electron is localized on one ^{93}Nb ($I = {}^9/_2$) nucleus. The uneven spacing in the decet is typical of a large hyperfine interaction coupled with a high nuclear spin, and the marked variation in line width across the manifold is characteristic of large anisotropy in both g and a.[31] The true extent of the anisotropies is revealed in the spectra taken at low temperature.

The ESR spectra of **2** and **3** at 110 K in frozen THF are shown in Figures 5 and 6, respectively. These spectra may be compared to that of copolymer-attached CpNbCl$_3$ obtained by Kilmer and Brubaker;[32] there is a close similarity. The spectra are typical of axially (or nearly axially) symmetric electronic doublets with g and the hyperfine tensors coparallel (or nearly so). Simulated spectra[33] were gen-

(30) Miller, D. A.; Bereman, R. D. *Coord. Chem. Rev.* **1973**, *9*, 107.
(31) Symons, M. C. R. *Chemical and Biochemical Aspects of Electron-Spin Resonance Spectroscopy*; Wiley: New York, 1978; Chapter 12.
(32) Kilmer, N. H.; Brubaker, C. H. *Inorg. Chem.* **1979**, *18*, 3283.

Table IV. ESR Parameters for $[CpNbCl(\mu\text{-}A)]_3(\mu_3\text{-}OH)(\mu_3\text{-}O)$ (A = Cl, OH; in Tetrahydrofuran Solution)

	A = Cl	A = OH
$g_\parallel$	1.9232	1.9049
$g_\perp$	1.9832	1.9800
g_{av}	1.9632	1.9550
g_{iso}	1.9632	1.9596
$a_\parallel^{93}$	649[a] (667[b])	658
$a_\perp^{93}$	303	299
a_{av}^{93}	418	419
a_{iso}^{93}	410	418
P_{exptl}[c]	372 (392[b])	379
a_{iso}	−404	−401
% d_{xy}	81 (86[b])	83
% s[d]	−6 (−6[b])	−6

[a] Hyperfine interactions a are in units of MHz. [b] Value for the second (with the less intense spectrum) isomer of **2** (A = Cl); other values indistinguishable from first (more intense) isomer. [c] Calculated (MHz) from the expressions given in the text, assuming that all hyperfine tensor components are negative. [d] Negative s spin density due to nuclear core polarization.

erated as a function of trial sets of components of g and $a(^{93}Nb)$ for both **2** (Figure 5) and **3** (Figure 6) until the closest visual match with the experimental spectrum was obtained. The best-fit tensors are given in Table IV.

Of the low-temperature spectra, that of **3** is less complicated. A good simulation (Figure 8) was readily achieved by using coparallel, axially symmetric g and $a(^{93}Nb)$ tensors (Table IV). There was no indication of hyperfine interactions from nuclei other than a single Nb, although the line width was quite large (≅30 G), suggesting the presence of unresolved hyperfine couplings or of the presence of more than one isomer (vide infra).

While the spectrum of the frozen solution of **2** (Figure 5) clearly arose from a species having parameters very similar to those of **3**, it showed a number of additional features, possibly because of the substantially lower line width (≅10 G). None of these extra features are attributable to nuclear hyperfine interactions. The most striking differences are the splitting in the intense $m_I = {}^3/_2$ perpendicular transition and the additional weak absorptions that accompany each of the parallel transitions. The latter are especially notable at the low-field end of the spectrum of **2**, where the parallel manifold is sharpest (Figure 5). This "splitting" in the parallel transitions is due to the presence of two very similar radicals or sites that differ slightly in their $a_\parallel^{93}$ values. These isomeric radicals are discussed below. A composite simulation for a 1:3 ratio of isomers, with the parameters listed in Table IV gave the best match with the experimental spectrum but did not accurately reproduce the $m_I = {}^3/_2$ perpendicular transition. We believe that the splitting in the perpendicular absorption is due to a small ^{93}Nb quadrupolar coupling which would, of course, influence perpendicular transitions only.[34] At the present time it is not possible to include such an interaction in the simulation program[33] for $I = {}^9/_2$.

The close similarity of the g and ^{93}Nb hyperfine tensors for **2** and **3** shows that their carriers have comparable electronic configurations. Inspection of the tensors for these species (Table IV) shows that they possess a single unpaired electron which is essentially localized in a d_{xy} orbital on the Nb(3) nucleus. Here the local axis is defined with respect to a pseudooctahedral Nb(3); the z axis runs

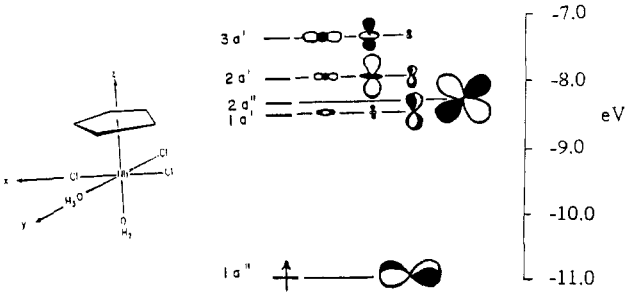

Figure 7. Molecular orbital energy levels for the model complex $[CpNbCl_3(H_3O)(H_2O)]^+$.

through the centroid of the C_5H_5 ring attached to Nb(3), Nb(3), and O(2), and the x and y axes are perpendicular to z, x in the direction of the Nb(3)–O(1) vector and y in the direction of Nb(3)–Cl(1). The proximity of the components of g to the free-spin value (2.0023) leaves no doubt that the species are electronic doublets, and the negative displacements from that value argue strongly for a d^1 configuration. Even more telling is the association of the smallest g value (the largest g shift) with the largest hyperfine component and their alignment along the z (parallel) direction. This is very reminiscent of the vanadyl ion, VO^{2+},[31] where the unpaired electron occupies a nonbonding d_{xy} orbital of the metal atom, and destabilization of the $d_{xz,yz}$ pair through strong π-interactions results in $g_\parallel < g_\perp < 2.0023$. Another analogy is copolymer-attached $CpNbCl_3$, which has a similar spectrum.[32] These observations and similarities eliminate assignment of the unpaired electron to d_{z^2}, for which the smallest g shift would be along z.

The contribution of the Nb(3) $4d_{xy}$ orbital to the singly occupied molecular orbital can be estimated from the ^{93}Nb hyperfine tensor and the theoretical expressions[35,36] for unit unpaired spin density:

$$a_\parallel = a_{iso} + P(-4/7 + \Delta g_\parallel + 3\Delta g_\perp/7)$$

$$a_\perp = a_{iso} + P(2/7 + 11\Delta g_\perp/14)$$

where P $(=\gamma_e\gamma_N\langle r^3\rangle)$ is the electronic–nuclear dipolar interaction parameter, which has been estimated as 457.3 MHz for ^{93}Nb.[36] The Δg terms are small corrections (≅10% in the present case), which represent the orbital contribution to the hyperfine interaction.[35] When P_{exp} and a_{iso} were estimated from these expressions (Table IV), all hyperfine components were assumed to be negative. The data clearly suggest that the unpaired electron is essentially localized in the d_{xy} orbital of one Nb nucleus. The estimates of 80% or more for the spin population $(=-100P_{exp}/P)$ in d_{xy} are undoubtedly upper limits because of the omission of relativistic corrections to P.[37] However, they agree with the estimates from the extended Hückel calculations described below.

The above conclusions allow us to locate, with reasonable certainty, the unpaired spin within the molecular framework. The crystallographic data suggest a low-spin ($S = {}^1/_2$) molecule with the single unpaired spin on Nb(3). The environment of Nb(3) could be regarded as a tetragonally distorted octahedron with Cp and μ_3-O as axial ligands, in which case the situation parallels that in VO^{2+}.[31,38,39] A

(33) Belford, R. L.; Nilges, M. J. *Computer Simulation of Powder Spectra*; EPR Symposium, 21st Rocky Mountain Conference, Denver, CO, 1979.
(34) Atherton, N. M. *Electron-Spin Resonance*; Wiley: New York, 1973; Chapter 7.
(35) Abragam, A.; Pryce, M. H. L. *Proc. R. Soc. London* **1951**, *A205*, 135. McGarvey, B. R. *Transition Met. Chem.* **1966**, *3*, 89.
(36) Morton, J. R.; Preston, K. F. *J. Magn. Reson.* **1978**, *30*, 577.
(37) Lionel, T.; Morton, J. R.; Preston, K. F. *J. Magn. Reson.* **1982**, *49*, 225.
(38) Morton, J. R.; Preston, K. F.; Vaills, J. P. *Can. J. Spectrosc.* **1988**, *33*, 43.
(39) Boyer, M. P.; LePage, Y.; Morton, J. R.; Preston, K. F.; Vuolle, M. J. *Can. J. Spectrosc.* **1981**, *26*, 181.

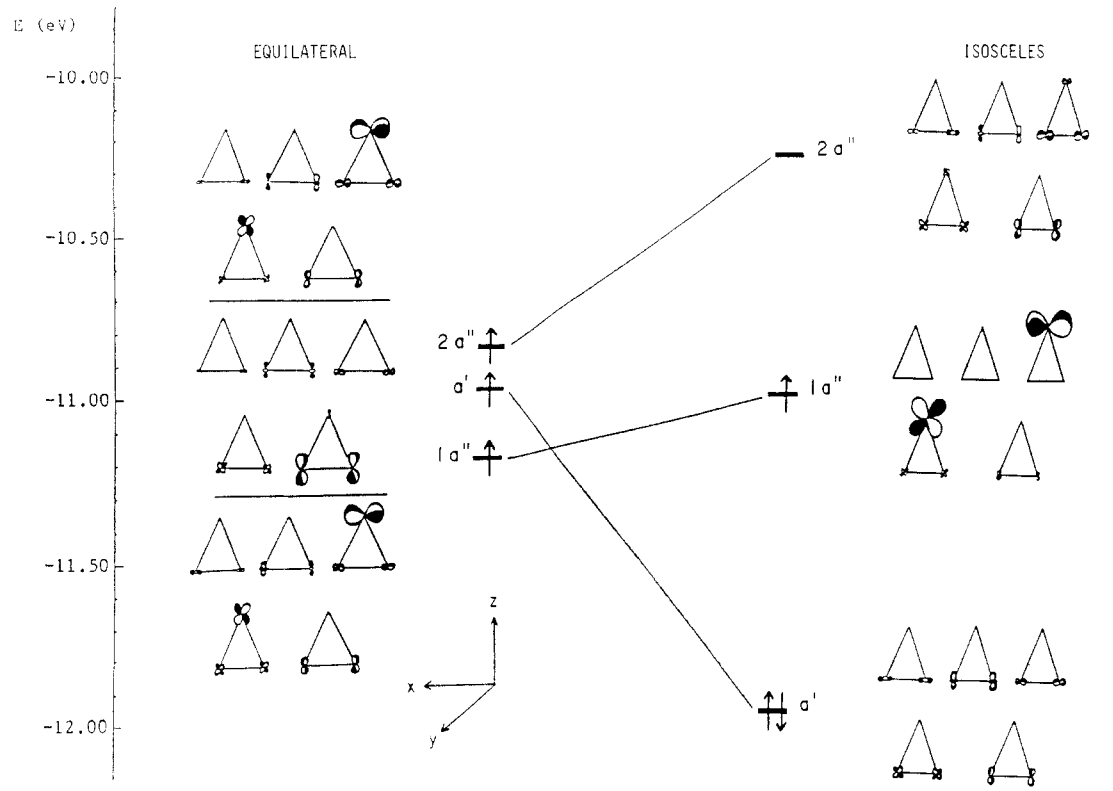

Figure 8. Contributions of the niobium d orbitals and energy levels of the three frontier orbitals of $[CpNbCl(\mu\text{-}Cl)]_3(\mu_3\text{-}OH)(\mu_3\text{-}O)$ with an equilateral triangular and with the observed isosceles triangular geometry.

more realistic approach is to begin with the C_{4v} bar-stool fragment $CpNbL_4$, whose orbital scheme has been described by Kubacek, Hoffmann, and Havlas,[40] and attach a further ligand along the z axis. We have performed extended Hückel calculations on $[CpNbCl_3(H_3O)(H_2O)]^+$, a rather esoteric cation but one that mimics the coordination about Nb(3) and also about the donor oxygen atoms in **2**. The results of these calculations for the d-orbital energy levels are shown in Figure 7. For a pure d_{xy} ground state, an empty $d_{x^2-y^2}$ level, and an empty degenerate $d_{xy,yz}$ pair, the g shifts would be given[34] by

$$\Delta g_{\parallel} = -8\lambda/\Delta_1 \qquad \Delta g_{\perp} = -2\lambda/\Delta_2$$

where λ is the spin–orbit coupling constant for Nb(IV) and Δ_1 and Δ_2 are the excitation energies of the empty levels, respectively. These relationships show the marked influence that even a remote x^2-y^2 level can exert on the value of $g_{\parallel}$. In the symmetry of **2** and **3** or of the hypothetical cation (C_s at best), the mixing of levels through spin–orbit interaction is even more complicated. Using the orbital compositions and energy levels predicted for $[CpNbCl_3(H_3O)(H_2O)]^+$ and the known[41] spin–orbit coupling constant for Nb(IV), we calculate $g_{xx} = 1.953$, $g_{yy} = 1.950$, and $g_{zz} = 1.876$, a tensor that closely matches the experimental tensors for **2** and **3**. The near-axiality of the g tensor in this type of radical is closely related to the proximity of the 1a′ and 2a″ levels (Figure 7), which originate with the erstwhile degenerate e pair in C_{4v}.

Electronic and Molecular Structure of $[CpNbCl(\mu\text{-}A)]_3(\mu_3\text{-}OH)(\mu_3\text{-}O)$. The plane results clearly localize the unpaired electron in a d_{xy} orbital on the Nb(3) atom of **2** and **3**, the local axis about Nb(3) being defined as above. The plane of this d_{xy} orbital makes an angle of approximately 45° to the plane of the Nb_3 ring. Curtis and Real[6] used the extended Hückel model for $[Cl_2Mo(\mu\text{-}Cl)]_3(\mu_3\text{-}S)_2$ (developed by Hoffmann and co-workers[42]) to explain the isosceles triangle and single unpaired electron of $[CpNbCl(\mu\text{-}Cl)]_3(\mu_3\text{-}OH)(\mu_3\text{-}O)$. The Curtis/Real model assigns the unpaired electron to an orbital localized completely in the plane of Nb_3. The reason for the discrepancy between the Curtis/Real model and the present results is that $[Cl_2Mo(\mu\text{-}Cl)]_3(\mu_3\text{-}S)_2$ is symmetrical (D_{3h}) and the metal is six-coordinate. In **2** the niobium is eight-coordinate and the symmetry is C_s, independent of whether the Nb_3 triangle is equilateral or isosceles. We performed extended Hückel calculations of the Hoffmann type using both an equilateral and an isosceles triangle for $[CpNbCl(\mu\text{-}Cl)]_3(\mu_3\text{-}OH)(\mu_3\text{-}O)$. The equilateral triangle had Nb–Nb distances of 3.275 Å and the isoceles triangle had Nb(1)–Nb(2) = 2.823 Å and Nb(1)–Nb(3) = Nb(2)–Nb(3) = 3.275 Å. The contributions of the Nb d orbitals to the three frontier molecular orbitals of $[CpNbCl(\mu\text{-}Cl)]_3(\mu_3\text{-}OH)(\mu_3\text{-}O)$ with both an equilateral and an isosceles triangle of Nb_3 are sketched in Figure 8; their relative energies are also shown in Figure 8, which shows clearly that the unpaired electron of **2** occupies a 1a″ orbital that is almost completely (>80%) localized on Nb(3). This 1a″ orbital is a hybrid of the in-plane d_{xz} (28%) and out-of-plane d_{xy} (52%) orbitals. Such a hybrid would make an angle of approximately 52° to the plane of Nb_3, which agrees with the ESR assignment. Note that the pair of electrons occupy an a′ orbital which is bonding between Nb(1) and Nb(2), though mainly π or δ in character.

There remains the question of why **2** adopts the isosceles triangular structure with one unpaired electron rather than the equilateral triangle with three. The energies of the three frontier orbitals in the equilateral triangular structure are very similar (Figure 8); the spread between 1a″ and

(40) Kubacek, P.; Hoffmann, R.; Havlas, Z. *Organometallics* **1982**, *1*, 180.

(41) Goodman, B. A.; Raynor, J. B. *Adv. Inorg. Chem. Radiochem.* **1970**, *13*, 135.

(42) Jiang, Y.; Tang, A.; Hoffmann, R.; Huang, J.; Lu, J. *Organometallics* **1985**, *4*, 27.

2a″ is 0.3310 eV. The extended Hückel calculations show that there is a large drop (0.9676 eV) in the energy of the bonding a′ orbital on going from the equilateral to the isosceles triangle but only a small increase in the energy of the antibonding 1a″ (0.1958 eV). The antibonding 2a″ increases more markedly in energy (0.5982 eV). The net gain in energy on going from the equilateral triangle with three unpaired electrons to the isosceles with one is large, 1.865 eV. Because of the low symmetry (C_s) of even an equilateral triangular $[CpNbCl(\mu\text{-}Cl)]_3(\mu_3\text{-}OH)(\mu_3\text{-}O)$, the Jahn–Teller distortion discussed by Hoffmann and co-workers[42] for $[Cl_2Mo(\mu\text{-}Cl)]_3(\mu_3\text{-}S)_2$ is not the reason for the large gain in energy in $[CpNbCl(\mu\text{-}Cl)]_3(\mu_3\text{-}OH)(\mu_3\text{-}O)$. The forbidden crossover advanced by Curtis and Real[6] to explain the location of the unpaired electron does not apply either, because the two frontier orbitals of lowest energy are not of the same symmetry in either an equilateral or isosceles triangular form of $[CpNbCl(\mu\text{-}Cl)]_3(\mu_3\text{-}OH)(\mu_3\text{-}O)$. We are left with the simple explanation that the energy gained through Nb–Nb bonding is larger than that to be gained through the decrease in Coulombic repulsion in an equilateral triangular high-spin (quartet) state. Shortening the Nb(1)–Nb(2) distance results in the bonding a′ orbital dropping to lower energy. To preserve the center of gravity, the antibonding a″ orbitals both go to higher energy. Because these antibonding orbitals are of the same symmetry, they repel one another, resulting in a large increase in energy for one of them and only a very small increase in the other.

Isomerism in $[CpNbCl(\mu\text{-}A)]_3(\mu_3\text{-}OH)(\mu_3\text{-}O)$. The ESR spectrum of **2** at 110 K clearly shows the presence of two radicals of very similar electronic structure (Figure 5); in essence, all absorptions appear as doublets. These doublets could not be simulated by any combination of nuclear hyperfine interactions (e.g. $^{35,37}Cl$) or g-tensor components, and we conclude that two isomeric radicals are present.

Two different types of isomerism may be envisaged for **2** and **3**. In the first the three edge-bridging Cl or OH ligands become terminal, one on each Nb atom. This isomerization may be fluxional in the same manner as is observed in many carbonyl clusters. The coordination number of the niobium would change from 8 in **2** and **3** to 7 in the unbridged form, and this would undoubtedly have a marked effect on the ESR parameters. Two lines of chemical evidence suggest that this type of isomerism is not taking place. First, attempts to replace the Cl ligands in **2** by OH^- were not successful on a molar scale; treatment of **2** with large quantities of water or OH^- leads to general decomposition. If **2** were undergoing the fluxional isomerism described, attack of OH^- at the seven-coordinate isomer would be expected to occur. Secondly, Maitlis and co-workers have demonstrated that the bridging hydride in $[Cp^*Rh(\mu\text{-}H)]_3(\mu_3\text{-}O)^+$ does not become terminal, and the activation energy for such a fluxionality, which would be a process very similar to that of the bridging Cl in **2**, is greater than 86 kJ mol^{-1}.[43]

The second type of isomerism of **2** is an intermolecular shift of the proton H(1) from O(1) to O(2). A similar shift could occur in **3**. Such a shift would be accompanied by shortening of the Nb–O(1) and lengthening of the Nb–O(2) distances, as well as less marked changes in the angles around the Nb atoms. The effective symmetry of $[CpNb(\mu\text{-}A)]_3(\mu_3\text{-}OH)(\mu_3\text{-}O)$ (C_s) is not changed by the movement of the proton, but because of the inequivalence of the two sides of the Nb_3 plane, a small change in the ESR parameters is expected. In the geometry shown in Figure 7 the proton moves from an equatorial to an axial position on isomerization. Therefore, one would anticipate a difference in the ^{93}Nb hyperfine interactions for the two isomers. The intermolecular transfer of a proton will be facilitated by the THF solvent. However, steric hindrance to the approach of THF on the side of the Nb_3 plane that bears two Cp rings will favor **2** (with H(1) attached to O(1)) as the more stable isomer.

The ESR spectra and their simulations support proton transfer as the isomerization process. In effect, the same radical is trapped in two different sites in a THF matrix. This is, in fact, the situation if one regards the proton transfer as taking place intermolecularly via the THF oxygen. The simulation suggests a ratio of 1:3 for the concentration of the isomers; we assign the more intense signal to the isomer shown in Figure 2, this being the least sterically hindered one. In this respect it is interesting to note that in $[CpNbCl(\mu\text{-}Cl)]_3(\mu_3\text{-}Cl)(\mu_3\text{-}O)$ the μ_3-oxygen atom is on the side of the Nb_3 plane carrying one Cp and two Cl ligands, the μ_3-chloride occupying the position of μ_3-O in **2**.[6] There is no hydrogen bonding in $[CpNbCl(\mu\text{-}Cl)]_3(\mu_3\text{-}Cl)(\mu_3\text{-}O)$.

Experimental Section

The starting materials $CpNbCl_4$ and Cp^1NbCl_4 were prepared by literature methods.[15] All other materials were reagent grade. Solvents (toluene, ether, THF, and hexane) were predried according to standard methods, stored under vacuum over MeLi, and distilled under vacuum. Water was doubly distilled and deoxygenated. Infrared spectra were measured on a Perkin-Elmer 683 instrument, ESR spectra on a locally modified version of the Varian E4 spectrometer, and NMR spectra on a Varian XL-200 multinuclear instrument. The ESR spectra were simulated by a computer program.[33] C, H, and Cl analyses were by the Beller Laboratorium, Göttingen, West Germany, zinc by atomic absorption, and molecular weights by the Mikroanalytisches Laboratorium, Engelskirchen, West Germany.

Hydrolysis of $CpNbCl_4$: Formation of $[CpNbL_4]_2(\mu\text{-}O)$. To a suspension of $CpNbCl_4$ (2.46 g, 8.2 mmol) in THF (100 cm^3) was added water (0.15 cm^3, 8.3 mmol). The solution changed rapidly from red-pink ($CpNbCl_4$, which is red-brown, forms a bright pink insoluble adduct with THF) to yellow-brown. The mixture was stirred at room temperature for 2 h and filtered and the filtrate reduced in volume to 50 cm^3 under vacuum. Addition of ether (100 cm^3) precipitated $[CpNbL_4]_2(\mu\text{-}O)$ as a yellow-brown solid (2.02 g). This mixture was used without further purification. The Cp^1 derivative was prepared analogously.

Reduction of $[CpNbL_4]_2(\mu\text{-}O)$ with Zinc Powder: Formation of $[CpNbCl(\mu\text{-}OH)]_3(\mu_3\text{-}OH)(\mu_3\text{-}O)$ (3). A suspension of $[CpNbL_4]_2(\mu\text{-}O)$ (2.64 g) in THF (100 cm^3) was treated with zinc powder (0.71 g). The color changed immediately from yellow-brown to red-brown. The mixture was stirred for 1 h at room temperature and filtered and the precipitate washed with THF until the washings were nearly colorless. The combined filtrates were reduced in volume to 50 cm^3, and ether (100 cm^3) was added. The red-brown solid obtained was recrystallized from THF/ether; yield 2.00 g. Anal. Calcd for $C_{34}H_{47}Nb_6Cl_7O_{12}$ ($[[CpNbCl(OH)]_3(OH)(O)]_2ZnCl(OH)(THF)$): C, 26.9; H, 3.1; Cl, 16.3; Zn, 4.3. Found: C, 26.5; H, 3.3; Cl, 16.6; Zn, 4.6. Mol wt: found (by osmometry in solution), 686; calcd for $[CpNbCl(OH)]_3(OH)(O)$, 664. ^1H NMR (THF-$^2H_8$): 6.65 ppm. Magnetic moment (Evans method): 1.33 μ_B (corrected for ligand and niobium diamagnetic contributions, by using the formula $[CpNbCl(OH)]_3(OH)(O)$: since the moment was measured in THF solution, it is presumed that the trinuclear clusters are not linked by Zn^{2+}). ESR: principal component (**3**), g_{iso} = 1.9596, $A_{iso}(^{93}Nb)$ = 418 MHz; minor component (**5**), g_{iso} = 1.9760, $A_{iso}(^{93}Nb)$ = 327 MHz (see Figures 3b and 6a). Infrared (Nujol mull): ν(OH) 3300–3400 cm^{-1} (vbr).

Reaction of $[CpNbL_4]_2(\mu\text{-}O)$ with Aluminum Powder: Formation of $[CpNbCl(\mu\text{-}Cl)]_3(\mu_3\text{-}OH)(\mu_3\text{-}O)\cdot THF$ and $[CpNb(H_2O)Cl_3]_2(\mu\text{-}O)\cdot 2THF\cdot 0.5Et_2O$. To a suspension of

(43) Nutton, A.; Bailey, P. M.; Maitlis, P. M. *J. Organomet. Chem.* **1981**, *213*, 313.

$[CpNbL_4]_2(\mu\text{-}O)$ (2.06 g) in THF (150 cm^3) was added aluminum powder (0.23 g) and the mixture stirred at room temperature for 2 days. The mixture gradually changed from pink to yellow-brown. The mixture was filtered and the precipitate washed with THF until the washings were nearly colorless. The combined filtrates were concentrated to 50 cm^3, and ether (50 cm^3) was added. Red-brown crystals of $[CpNbCl(\mu\text{-}Cl)]_3(\mu_3\text{-}OH)(\mu_3\text{-}O)\cdot THF$, which were suitable for X-ray diffraction, formed over 6 days. At the same time yellow crystals of $[CpNb(H_2O)Cl_3]_2(\mu\text{-}O)\cdot 2THF\cdot 0.5Et_2O$ also formed. The two compounds were separated manually. Data for $[CpNbCl(\mu\text{-}Cl)]_3(\mu_3\text{-}OH)(\mu_3\text{-}O)\cdot THF$ are as follows. Mass spectrum (FAB, negative ion, ^{35}Cl, m/e): 717 (M^-); 682 ($M^- - Cl$); 652 ($M^- - Cp$); 617 ($M^- - Cp - Cl$). Infrared (Nujol mull): ν(OH) 3300 (vbr, w), $\delta(Nb_3OH)$ 1067 (m) cm^{-1}. Magnetic moment (Evans method): 1.39 μ_B (corrected for ligand and Nb diamagnetism). ESR (293 K): 10 lines, $g_{iso} = 2.011$, $A_{iso}(^{93}Nb) = 410$ MHz (see also Table IV and Figures 3a and 5a).

Reaction of $[Cp^1NbL_4]_2(\mu\text{-}O)$ with Aluminum Powder: Formation of $Cp^1_4Nb_5Cl_5(OH)_9O(THF)_2$ (5). Aluminum dust (0.083 g) was added to a suspension of $[Cp^1NbL_4]_2(\mu\text{-}O)$ (1.757 g) in THF (100 cm^3). The mixture was stirred for 8 days, during which time the color changed from brown to bright green, and then filtered. The solid was washed with THF (20 cm^3), and the combined filtrates were concentrated to approximately 30 cm^3. The concentrated solution was frozen (liquid nitrogen) and then layered with approximately 100 cm^3 of Et_2O, giving a brown precipitate. This was collected by filtration and recrystallized from THF/ether (50 cm^3/75 cm^3); yield 0.33 g, 21%. Anal. Calcd for $C_{32}H_{53}Cl_5Nb_5O_{12}$: C, 30.2; H, 4.2; Cl, 13.9. Found: C, 29.2; H, 3.5; Cl, 14.4. Mol wt (osmometric, THF solution): found, 1230; calcd, 1271.6. Magnetic moment (Evans method, THF solution): 1.86 μ_B. ESR spectrum (295 K, THF solution): 10 lines, $g_{iso} = 1.9767$, $A_{iso}(^{93}Nb) = 322.3$ MHz. Infrared: ν(OH) 3300 cm^{-1} (weak, br). ^1H NMR (THF-$^2H_8$ solution): 6.38 (br m, $C_5H_4CH_3$) 2.38 ppm (br s, $C_5H_4CH_3$). Mass spectrum (positive ion, EI, ^{35}Cl, m/e): 1265–1261 (M^+); 1247–1243 ($M^+ - OH$); 1230–1226 ($M^+ - 2OH$); 1214–1210 ($M^+ - 3OH$); 1118 ($M^+ - 2THF$).

Green-brown poorly formed crystals were obtained on recrystallization of **5** from toluene. They were of the monoclinic class, with $a = 11.765$ (2) Å, $b = 19.175$ (4) Å, $c = 22.863$ (4) Å, $\beta = 99.92$ (1)°, and space group $P2_1/c$. The crystals diffracted weakly, and significant data could be obtained only to $2\theta = 44°$. The intensities of 6650 unique reflections were measured, of which 2491 (37%) had $I > 2.5\sigma(I)$. Using these reflections, it was possible to obtain the positions of the five Nb atoms, the six bridging oxygen atoms of the adamantane-like unit, and the bridging oxygen to the unique Nb (see Figure 4). It was then evident that the terminal Cl and OH ligands were disordered among each another and that there was a molecule of solvent (toluene) in the asymmetric unit. These problems were reasonably, though not necessarily correctly, overcome by partitioning the various sites between Cl, O, and C. Further refinement readily gave the position of one Cp^1 ring, but the three other rings and the two THF groups, while present as regions of high electron density, could not be accurately located or refined. The final R achieved was 0.14.

Crystal and Refinement Data for $[CpNbCl(\mu\text{-}Cl)]_3(\mu_3\text{-}OH)(\mu_3\text{-}O)\cdot THF$ (2). Crystals were obtained by setting aside a solution of **2** in THF/ether for 6 days. The crystals were coated with air-free "Apiezon" grease and mounted in sealed tubes under argon. Space group symmetry, cell dimensions, and intensity data were collected from a crystal of dimensions 0.36 × 0.28 × 0.18 mm with use of an Enraf-Nonius CAD-4 diffractometer. Crystal data: $C_{19}H_{24}Cl_6Nb_3O_3$, $M_r = 791.56$, monoclinic, $P2_1/c$, $a = 9.966$ (1) Å, $b = 12.471$ (2) Å, $c = 20.321$ (2) Å, $\beta = 93.86$ (1)°, $V = 2519.9$ (3) Å^3, $Z = 4$, $F(000) = 1548$, $D_{calc} = 2.09$ Mg m^{-3}, λ(Mo Kα) = 0.710 73 Å, μ(Mo Kα) = 21.5 cm^{-1}. Cell dimensions were determined from 30 reflections with $30 < 2\theta < 40°$, and the intensities of 4406 unique reflections were measured to $2\theta = 50°$ by the $\theta/2\theta$ scan method, of which 3507 were judged as observed by the criterion that $I > 2.5\sigma(I)$. No absorption correction was applied. The structure was solved by direct methods[44] and refined by the NRCVAX program.[45] The function minimized was $\sum w(\Delta F)^2$, with a weighting scheme of the form $w = 1/(\sigma(F)^2 + 0.001F^2)$ with σ determined from counting statistics. The final R ($=\sum\Delta|F|/\sum|F_o|$) was 0.027, R_w ($=(\sum w(\Delta F)^2)^{1/2}$) was 0.038, and the goodness of fit was 0.95, with use of 307 parameters. The maximum value of Δ/σ in the final cycle was 1.97. In a final difference synthesis the highest peak was 0.5 e Å^{-3} and the deepest hole was −0.49 e Å^{-3}. Scattering factors were taken from ref 46 and were corrected for both the real and the imaginary parts of the anomalous dispersion. Hydrogen atoms were included in calculated positions (C–H = 0.96 Å, sp^2 hybridization) with fixed isotropic thermal

Table V. Atomic Parameters for the Non-Hydrogen Atoms of $[CpNbCl(\mu\text{-}Cl)]_3(\mu_3\text{-}OH)(\mu_3\text{-}O)\cdot THF$ (Esd's in Parentheses)

	x	y	z
Nb(1)	0.15906 (4)	0.27497 (3)	0.200869 (18)
Nb(2)	0.43309 (4)	0.23483 (3)	0.183145 (18)
Nb(3)	0.27147 (4)	0.37360 (3)	0.067805 (18)
O(1)	0.2579 (3)	0.21281 (22)	0.11505 (13)
O(2)	0.3126 (3)	0.37025 (22)	0.16851 (14)
Cl(1)	0.04437 (12)	0.39410 (10)	0.11196 (6)
Cl(2)	0.51897 (11)	0.33232 (10)	0.08311 (6)
Cl(3)	0.27813 (12)	0.10444 (9)	0.23654 (6)
Cl(4)	−0.02118 (11)	0.15440 (10)	0.16015 (7)
Cl(5)	0.51021 (12)	0.07512 (9)	0.12593 (6)
Cl(6)	0.30567 (14)	0.56561 (10)	0.07837 (7)
C(11)	0.2035 (7)	0.3740 (12)	0.3013 (4)
C(12)	0.1062 (13)	0.4268 (6)	0.2649 (4)
C(13)	−0.0016 (8)	0.3684 (9)	0.2606 (4)
C(14)	0.0190 (11)	0.2791 (8)	0.2927 (4)
C(15)	0.1483 (13)	0.2768 (9)	0.3192 (3)
C(21)	0.6246 (6)	0.3388 (6)	0.2258 (3)
C(22)	0.5313 (6)	0.3488 (5)	0.2714 (3)
C(23)	0.5111 (7)	0.2488 (7)	0.2977 (3)
C(24)	0.5937 (8)	0.1771 (5)	0.2685 (3)
C(25)	0.6633 (5)	0.2311 (7)	0.2239 (4)
C(31)	0.3018 (6)	0.2714 (4)	−0.02661 (24)
C(32)	0.3401 (6)	0.3759 (5)	−0.04383 (24)
C(33)	0.2255 (6)	0.4407 (4)	−0.04687 (25)
C(34)	0.1155 (6)	0.3775 (4)	−0.03149 (23)
C(35)	0.1628 (5)	0.2719 (4)	−0.01951 (23)
O(3)	0.8094 (3)	0.5322 (3)	0.45168 (17)
C(1)	0.8645 (8)	0.4471 (5)	0.4156 (4)
C(2)	0.8019 (11)	0.3492 (6)	0.4347 (6)
C(3)	0.7240 (16)	0.3707 (7)	0.4867 (7)
C(4)	0.7318 (7)	0.4865 (5)	0.5017 (3)
H(1)	0.233 (6)	0.150 (5)	0.091 (3)

Table VI. Atomic Parameters for the Non-Hydrogen Atoms of $[CpNb(H_2O)Cl_3]_2(\mu\text{-}O)\cdot 2THF\cdot 0.5Et_2O$ (Esd's in Parentheses)

	x	y	z
Nb(1)	0.90584 (6)	0.10925 (11)	0.61897 (9)
O(1)	1	0.1186 (11)	$^3/_4$
O(2)	0.9004 (4)	−0.0346 (8)	0.7079 (6)
Cl(1)	0.78472 (18)	0.0224 (3)	0.4963 (3)
Cl(2)	0.85191 (19)	0.2094 (4)	0.6986 (3)
Cl(3)	0.95434 (19)	−0.0619 (3)	0.5764 (3)
C(11)	0.8993 (9)	0.1722 (17)	0.4654 (12)
C(12)	0.8479 (8)	0.2351 (17)	0.4647 (14)
C(13)	0.8842 (11)	0.3124 (15)	0.5534 (17)
C(14)	0.9580 (10)	0.2908 (14)	0.6033 (12)
C(15)	0.9663 (8)	0.2069 (14)	0.5514 (13)
O(21)	0.7095 (5)	0.6149 (9)	0.2901 (7)
C(22)	0.7372 (11)	0.7193 (17)	0.3459 (16)
C(23)	0.8163 (14)	0.698 (3)	0.4198 (23)
C(24)	0.8370 (10)	0.5945 (20)	0.3915 (17)
C(25)	0.7676 (9)	0.5421 (17)	0.3075 (13)
O(3)	0	0.4536 (22)	$^1/_4$
C(31)	0.036 (3)	0.383 (3)	0.237 (3)
C(32)	0.0591 (22)	0.407 (3)	0.188 (3)

(44) Main, P.; Fiske, S. J.; Hull, S. E.; Lessinger, L.; Germain, G.; Declerq, J. P.; Woolfson, M. M. MULTAN-80; University of York: York, England, 1980.

(45) Gabe, E. J.; Lee, F. L.; LePage, Y. In *Crystallographic Computing*; Sheldrick, G. M., Kruger, C., Goddard, R., Eds.; Clarendon Press: Oxford, England, 1980; Vol. 3, p 167.

(46) *International Tables for X-ray Crystallography*; Kynoch Press: Birmingham, England, 1974; Vol. IV.

parameters, except for H(1), whose position was taken from a difference synthesis and refined. All non-hydrogen atoms were refined anisotropically. Positional parameters are given in Table V and important distances and angles in Table II; full details have been deposited as supplementary material.

Crystal and Refinement Data for $[CpNb(H_2O)Cl_3]_2(\mu$-O)·2THF·0.5Et$_2$O (1). Crystals were obtained as described and were mounted as described for **2** above. Crystal data: dimensions 0.36 × 0.28 × 0.07 mm, $C_{20}H_{35}Cl_6Nb_2O_{5.5}$, M_r = 762.05, monoclinic, $C2/c$, a = 22.105 (4) Å, b = 11.366 (1) Å, c = 15.563 (2) Å, β = 124.707 (9)°, V = 3214.5 (7) Å^3, Z = 4, $F(000)$ = 1532, D_{calc} = 1.57 Mg m^{-3}, μ(Mo Kα) = 12.1 cm^{-1}; cell dimensions from 25 reflections with 30 < 2θ < 40°; intensities of 4201 reflections measured to 2θ = 45°, of which 1444 had $I > 2.5\sigma(I)$; no absorption correction; refinement as for **2**; final R = 0.056, R_w = 0.076, goodness of fit 2.22, for 165 parameters; maximum Δ/σ 0.21; highest peak 0.83 e Å^{-3}, deepest hole −0.55 e Å^{-3}. Positional parameters are given in Table VI and important distances and angles in Table I; full details have been deposited as supplementary material.

Acknowledgments. We thank the Natural Sciences and Engineering Research Council of Canada, the Imperial Oil Research Fund, and the donors of the Petroleum Research Fund, administered by the American Chemical Society, for financial support of this work. Rod McGregor is thanked for assistance with the ESR spectra, Ljubica Bottomley for the atomic absorption analyses, Andrew Sharpe for the preparation of starting materials, and Friedrich Grein for assistance with the extended Hückel calculations.

Registry No. 1, 112942-46-8; 1·2THF·0.5Et$_2$O, 126752-69-0; 2, 126752-72-5; 2·THF, 126821-22-5; 3, 126752-70-3; 5, 126752-71-4; $CpNbCl_4$, 33114-15-7.

Supplementary Material Available: Figures showing the positions of the adduct molecules, tables giving the hydrogen atom positions, thermal parameters, bond lengths and angles, and contributions of the Nb d orbitals to the frontier orbitals of 1 and 2, and a table giving the distances from the least-squares planes of 2 (19 pages); tables of the observed and calculated structure factors for 1 and 2 (45 pages). Ordering information is given on any current masthead page.

Chemistry of Carbon Monoxide Free Cyclopentadienylvanadium(I) Alkene and Alkyne Complexes

Bart Hessen, Auke Meetsma, Fré van Bolhuis, and Jan H. Teuben*

Groningen Center for Catalysis and Synthesis, Department of Chemistry, Rijksuniversiteit Groningen, Nijenborgh 16, 9747 AG Groningen, The Netherlands

Göran Helgesson and Susan Jagner

Department of Inorganic Chemistry, Chalmers University of Technology, S-412 96, Göteborg, Sweden

Received February 5, 1990

The compounds CpV(L)(PMe$_3$)$_2$ (L = η^2-ethene (**2**), η^2-alkyne) form a new class of highly reactive CO-free CpV^I complexes. Paramagnetic **2** was prepared from CpVCl(PMe$_3$)$_2$ and 0.5 mol of BrMg(CH$_2$)$_4$MgBr. An X-ray structure determination shows a relatively short ethene C=C distance of 1.365 (5) Å. The η^2-alkyne complexes are readily available by Mg reduction of CpVCl$_2$(PMe$_3$)$_2$ in the presence of the alkyne. The X-ray structure of CpV(η^2-PhC≡CPh)(PMe$_3$)$_2$ (**4**) shows the alkyne ligand to be asymmetrically oriented relative to the other ligands in the complex. The ethene ligand in **2** is readily replaced by CO or PhC≡CPh. 2,2′-Bipyridine displaces a phosphine as well to produce the paramagnetic CpV(η^2-bpy)PMe$_3$ (**5**). C,C coupling is observed in the reaction of **2** with CO$_2$ to form the vanadalactone CpV[CH$_2$CH$_2$C(O)O]PMe$_3$ (**6**). PhSSPh oxidatively adds to **2** to form [CpV(μ-SPh)$_2$]$_2$. 1-Hexene is slowly catalytically dimerized by **2**. The alkyne complex **4** reacts with various hydrocarbon substrates through initial phosphine loss and subsequent C,C coupling. With 1,3-butadiene the hexadienediyl complex CpV(η^1,η^3-C$_2$Ph$_2$C$_4$H$_6$)PMe$_3$ (**9**) is formed. With ethene 2:1 cotrimerization with the alkyne ligand occurs to produce an η^4-diphenylhexadiene complex, CpV[η^4-CH$_2$=CHC(Ph)=C(Ph)Et]PMe$_3$ (**10**), which was characterized by X-ray diffraction. With 2-butyne, **4** reacts to give CpV(η^2-MeC≡CMe)(η^2-PhC≡CPh)PMe$_3$ (**13**), which subsequently forms the metallacycle CpV(C$_4$Me$_2$Ph$_2$)PMe$_3$ (**14**). An X-ray structure determination shows **14** to have a bent metallacyclopenta-1,3,5-triene structure (formally an V(V) dicarbene) with V=C bond distances of 1.891 (3) and 1.893 (3) Å. Analogous bicyclic products are formed through reduction of CpVCl$_2$(PMe$_3$)$_2$ in the presence of diynes. A summary of the crystal data is as follows: for **2**, *Pbca*, a = 12.351 (3) Å, b = 15.526 (4) Å, c = 16.948 (3) Å (130 K), Z = 8; for **4**, $P2_1/n$, a = 8.249 (2) Å, b = 17.619 (2) Å, c = 16.278 (2) Å, β = 100.61 (2)° (130 K), Z = 4; for **10**, $P\bar{1}$, a = 8.875 (3) Å, b = 9.589 (2) Å, c = 15.081 (6) Å, α = 90.95 (3)°, β = 91.54 (3)°, γ = 117.44 (2)° (130 K), Z = 2; for **14**, $P2_12_12_1$, a = 12.957 (3) Å, b = 19.205 (5) Å, c = 9.155 (2) Å (170 K), Z = 4.

Introduction

The organometallic chemistry of vanadium(I) has hitherto been based mainly on CpV(CO)$_4$.[1] CO ligands in this compound can be photochemically or thermally replaced by one or more Lewis-base type ligands. In this way, a range of CpV(L)$_n$(CO)$_{4-n}$ (L = PR$_3$,[2] CS,[3] RC≡CR′ (=2L),[4]

(1) Fischer, E. O.; Haffner, W. *Z. Naturforsch.* **1954**, *9B*, 503.

(2) (a) Strohmeier, W.; Müller, F.-J. *Chem. Ber.* **1967**, *100*, 2812. (b) Rehder, D. *J. Magn. Reson.* **1977**, *25*, 177. (c) Alway, D. G.; Barnett, K. W. *Inorg. Chem.* **1980**, *19*, 779.

(3) Rajan, S. *Indian J. Chem., Sect. A* **1977**, *15*, 920.

0276-7333/90/2309-1925$02.50/0